ACCEPTED VERSION

Kerrie L. May, Marcin Grabowicz, Steven W. Polyak and Renato Morona
Self-association of the Shigella flexneri IcsA autotransporter protein,
Microbiology, 2012; 158(7):1874-1883

http://hdl.handle.net/2440/73371

1   **Title:** Self-association of the *Shigella flexneri* IcsA autotransporter protein

2

3   **Authors:** Kerrie L. May [1]†‡, Marcin Grabowicz[1]†§, Steven W. Polyak[2] and Renato

4   Morona[1]*.

5

6   [1]Discipline of Microbiology and Immunology, School of Molecular and Biomedical Science,

7   University of Adelaide, South Australia, Australia. [2]Discipline of Biochemistry, School of

8   Molecular and Biomedical Science, University of Adelaide, South Australia, Australia.

9

10   **Running title:**

11   IcsA self-association

12

13

14   * Corresponding author: Discipline of Microbiology and Immunology, School of Molecular

15   and Biomedical Science, University of Adelaide, South Australia 5005, Australia. Phone: 61-

16   8-83134151. Fax: 61-8-83137532. Email: renato.morona@adelaide.edu.au

17   † K.L.M. and M.G. contributed equally to this work.

18   ‡ Present address: School of Environmental and Biological Sciences, Rutgers University,

19   New Brunswick, NJ 08901.

20   § Present address: Department of Molecular Biology, Princeton University, Princeton, NJ

21   08544.

22

23   * To whom correspondence should be addressed. E-mail: renato.morona@adelaide.edu.au

24

25   Word count: 4,656

26   Table and figure count: 6

27

28

29 **ABSTRACT**

30 The IcsA autotransporter protein is a major virulence factor of the human intracellular

31 pathogen *Shigella flexneri*. IcsA is polarly distributed in the outer membrane of *S. flexneri*

32 and interacts with components of the host actin-polymerization machinery to facilitate

33 intracellular actin-based motility and subsequent cell-to-cell spreading of the bacterium. We

34 sought to characterize the biochemical properties of IcsA in the bacterial outer membrane.

35 Chemical cross-linking data suggested that IcsA exists in a complex in the outer membrane.

36 Furthermore, reciprocal co-immunoprecipitation of differentially epitope-tagged IcsA

37 proteins indicated that IcsA is able to self-associate. The identification of IcsA linker-

38 insertion mutants that were negatively dominant provided genetic evidence of IcsA-IcsA

39 interactions. From these results, we propose a model whereby IcsA self-association facilitates

40 efficient actin-based motility.

41

INTRODUCTION

Shigella spp. are highly adapted human pathogens that cause bacillary dysentery and

extensive global morbidity and mortality (Levine *et al.*, 2007). Ingested *Shigellae* invade

colonic epithelial cells, where they multiply within the host cell cytoplasm and become

motile via the polymerization of host actin in a process termed actin-based motility (ABM)

(Suzuki *et al.*, 1996; 1998; 2002). Motile bacteria are able to infect adjacent cells, enabling

the lateral spread of the focus of infection throughout the epithelium. Actin polymerization is

initiated by the polarly distributed *Shigella* IcsA (VirG) protein (Bernardini *et al.*, 1989; Lett

et al., 1988), which recruits the host neural Wiskott-Aldrich syndrome protein (N-WASP), a

key regulator of the actin cytoskeleton (Goldberg, 2001; Snapper *et al.*, 2001; Suzuki *et al.*,

1998). N-WASP and other members of the Wiskott-Aldrich syndrome protein (WASP)

family function as a link between signalling pathways and *de novo* actin polymerization by

recruiting the actin polymerizing complex Arp2/3, initiating actin polymerization-driven host

cell motility and morphological changes (Miki & Takenawa, 2003; Yarar *et al.*, 1999). IcsA

is essential for ABM and thus *S. flexneri* virulence (Kotloff *et al.*, 1996; 2002; Lett *et al.*,

1988; Makino *et al.*, 1986; Sansonetti *et al.*, 1991).

IcsA is a member of the autotransporter (AT) family of proteins, which is the largest

family of extracellular proteins in Gram-negative bacteria (Pallen *et al.*, 2003). A prototypical

AT protein consists of an N-terminal signal sequence that facilitates export across the inner-

membrane; an internal passenger domain that exerts the effector function; and a C-terminal

translocation domain required to direct export of the protein across the outer-membrane (OM)

via the Bam complex, and to form a β-barrel OM anchor for the extracellular passenger

domain (Henderson *et al.*, 2004; Jain & Goldberg, 2007; Peterson *et al.*, 2010).

A distinct sub-family of ATs has been shown to be trimeric and IcsA is related to a

subgroup of self associating ATs (SAATs) that mediate bacterial aggregation and biofilm

formation (Cotter *et al.*, 2005; Klemm *et al.*, 2006; Meng *et al.*, 2011). Emerging evidence

suggests that a subset of conventional ATs are capable of oligomerisation in the OM. In these

proteins, oligomerization is facilitated either through interactions between adjacent effector

70   domains (Gangwer *et al.*, 2007; Swanson *et al.*, 2009; Xicohtencatl-Cortes *et al.*, 2010), or

71   translocation domains (Marín *et al.*, 2010; Müller *et al.*, 2005; Veiga *et al.*, 2002). How

72   broadly applicable oligomerisation might be within the large AT family of proteins remains

73   to be determined. Indeed, some ATs have specifically been shown to exist as monomers

74   (Hritonenko *et al.*, 2006; Marín *et al.*, 2010), and crystal structures of translocation domains

75   obtained from EspP and NalP suggest a monomeric existence (Barnard *et al.*, 2007; Oomen *et*

76   *al.*, 2004). The biological significance of AT oligomerization remains unclear. IcsA has not

77   been previously investigated in this regard.

78   The aim of our study was to investigate the state of IcsA in the OM environment,

79   which is fundamental to understanding the interaction of IcsA with host proteins such as N-

80   WASP, and to *S. flexneri* virulence. In this study, we have shown that IcsA is present within a

81   complex in the OM, and detected the existence of direct IcsA-IcsA interactions within this

82   complex. The identification of negative-dominant IcsA mutants that influenced *S. flexneri*

83   plaque formation, and hence intercellular spreading, provided genetic evidence of direct

84   IcsA-IcsA interaction, and demonstrated the functional relevance of IcsA self-association.

85

86   **METHODS**

87   **Bacterial strains and Plasmids.** The strains and plasmids used in this study are listed in

88   Table 1.

89   **Growth media and growth conditions.** *S. flexneri* strains were grown from a Congo-Red-

90   positive colony as previously described (Morona *et al.*, 2003). All bacterial strains were

91   routinely cultured in Luria Bertani (LB) media. Bacteria were grown in media with

92   antibiotics for 16 h with aeration then sub-cultured 1:50 and grown to mid exponential-phase

93   by incubation with aeration for 2 h at 37°C. Where appropriate, media were supplemented

94   with ampicillin (100 µg ml^{-1}), chloramphenicol (25 µg ml^{-1}), kanamycin (50 µg ml^{-1}),

95   tetracycline (50 µg ml^{-1}). Mueller-Hinton broth and agar were used to culture strains in the

96   presence of trimethoprim (10 µg ml^{-1}).

97   **DNA methods.** *Escherichia coli* K-12 strain DH5α was used for routine cloning and general

98   cloning techniques, and PCR and DNA sequencing were performed as described previously

99   (May & Morona, 2008).

100   **Chemical cross-linking.** Cross-linking with dithio-bis(succinimidylpropionate) (DSP;

101   Pierce) was performed as described previously (Thanabalu *et al.*, 1998). Mid exponential-

102   phase cultures were washed in buffer (120 mM NaCl, 20 mM sodium phosphate pH 7.2) and

103   DSP was added to each sample at a final concentration of 0.2 mM in the same buffer.

104   Samples were incubated for 30 min at 37°C. Cross-linking was then quenched with 20 mM

105   Tris pH 7.5, samples were washed in buffer, resuspended in SDS-PAGE sample buffer

106   (Lugtenberg *et al.*, 1975) either with or without β-mercaptoethanol. Samples were then

107   heated to 60°C for 5 min, prior to being resolved by SDS-PAGE. Cross-linking of cells from

108   strains RMA2205, RMA2208, RMA2209, was performed as above, except that after

109   quenching, the cells were lysed by passage through a French pressure cell; the lysate was

110   centrifuged at 100,000×*g* for 1 h, and the pelleted whole membranes resuspended in SDS-

111   PAGE sample buffer either with or without β-mercaptoethanol. Formaldehyde cross-linking

112   was performed as described previously (Prossnitz *et al.*, 1988). Mid-exponential phase

113   bacteria were washed in 10 mM K_2HPO_4/KH_2PO_4 buffer and resuspended and formaldehyde

114   added at a final concentration 0.5% and incubated for 1 h at RT. Samples were then washed

115   once again as above and resuspended in SDS-PAGE sample buffer. Aliquots of each sample

116   were heated at either 60°C for 10 min or 100°C for 20 min, prior to SDS-PAGE.

117   **Construction of plasmids**

118   pKMRM252 was constructed by sub-cloning the *Eco*RI-*Sal*I fragment of pIcsA encoding

119   IcsA$_{WT}$ into likewise digested pBBR1MCS-2. FLAG and BIO tagged derivatives of IcsA

120   were constructed as follows. Complementary oligonucleotides (Table 2) encoding either the

121   FLAG epitope (IcsA-FLAG-F1, IcsA-FLAG-R1; DYKDDDDK) or the BIO sequence (KM1-

122   BIO-F, KM1-BIO-R; GLNDIFEAQKIEWH) were annealed as described previously

123   (Enninga *et al.*, 2005). The resultant dsDNA possessed *Not*I compatible 5' overhangs, and

124   was ligated into the unique *Not*I site within the linker-insertion of pKMRM1, producing

125 plasmids pKMRM250 (encoding $icsA_{i87::FLAG}$) and pMG55 (encoding $icsA_{i87::BIO}$). To enable

126 co-expression with pMG55, the *Eco*RI-*Sal*I fragment of pKMRM250 encoding $icsA_{i87::FLAG}$

127 was sub-cloned between the *Eco*RI and *Sal*I sites of the compatible plasmid pBBR1MCS-2,

128 producing plasmid pKMRM270. We confirmed that $IcsA_{i87::FLAG}$ and $IcsA_{i87::BIO}$ were

129 functionally comparable to $IcsA_{WT}$ by introducing either pKRM250 or pMG55 into

130 RMA2041 (Table 1) and performing plaque assays (data not shown).

131 **Reciprocal co-purification of FLAG- and BIO-tagged IcsA.**

132 *E. coli* UT5600 was transformed with pKMRM270 and pMG55, enabling co-expression of

133 $IcsA_{i87::FLAG}$ and $IcsA_{i87::BIO}$ resulting in in strain MG157. Control strains were also generated

134 that expressed untagged $IcsA_{i87}$ [pKMRM1] with either $IcsA_{i87::FLAG}$ [pKRM270] (MG250)

135 or $IcsA_{i87::BIO}$ [pMG55] (MG251). Strains MG157, MG250, and MG251 additionally carried

136 pCY216 (Chapman-Smith *et al.*, 1994).

137 Cultures (5 L) of MG157, MG250, and MG251 were grown 16 h at 30ºC and

138 extraction of outer membrane proteins from each strain was performed at 4ºC as previously

139 described (Veiga *et al.*, 2002). Briefly, bacteria were pelleted, resuspended in TN buffer (20

140 mM Tris-HCl pH 8.0, 10 mM NaCl), lysed by passage in a French pressure cell at 12,000 psi,

141 and centrifuged at $100,000 \times g$ for 1 h. The pellet was solubilised in TN buffer supplemented

142 with 1.5% (v/v) Triton X-100 (Sigma) for 30 min, and centrifuged at $100,000 \times g$ for 1 h. The

143 resulting pellet was solubilised in TN buffer supplemented with 1% (w/v) Zwittergent 3-14

144 (Calbiochem) for 30 min, and centrifuged at $100,000 \times g$ for 1 h. The supernatant containing

145 solubilised outer-membrane proteins was collected, and diluted to 0.1% (w/v) Zwittergent 3-

146 14 with TN buffer. Solubilised material was then used in affinity purification using FLAG

147 M2 resin (Sigma) or MyOne streptavidin T1 Dynabeads (Invitrogen). Samples and beads or

148 resin were incubated overnight at 4ºC, washed six times for 1.5 h in 8 ml TN buffer

149 containing 0.1% (w/v) Zwittergent 3-14. Proteins were eluted in SDS-PAGE sample buffer

150 from FLAG M2 resin; streptavidin-Dynabeads were heated at 100ºC for 5 min to release

151 bound protein, pelleted at $16,000 \times g$ for 5 min, and the supernatant then diluted in SDS-PAGE

152 sample buffer for electrophoresis.

SDS-PAGE and Western blotting. Samples were separated on 7.5% or 12% SDS-PAGE gels and transferred to a nitrocellulose membrane. The membrane was blocked for 1 h in TTBS (Tris-buffered saline, 0.05% Tween-20) containing 5% skim milk and incubated with either rabbit anti-IcsA polyclonal antibody (Van Den Bosch *et al.*, 1997), streptavidin-HRP (Chemicon), or with rabbit anti-FLAG M2 (Sigma) in TTBS overnight. After three 10 min washes in TTBS the membrane was incubated with horseradish peroxidase (HRP)-conjugated goat anti-rabbit or a HRP-conjugated goat anti-mouse secondary antibodies (Biomediq DPC) for 2 h, washed three times in TTBS, then three times in Tris-buffered saline. The membrane was incubated with Chemiluminescence Substrate (Sigma) for 1 min. Chemiluminescence was detected by exposure of the membrane to X-ray film (AGFA) and the film was developed using a Curix 60 automatic X-ray film processor (AGFA).

Plaque assays. Plaque assays were performed with HeLa cells as described previously (May & Morona, 2008). Briefly, HeLa cells were maintained in MEM, 10% FCS with penicillin and streptomycin and grown to confluence overnight in 6 well trays. HeLa cells were washed twice with Dulbecco's PBS (D-PBS) and once in DMEM prior to inoculation with mid exponential-phase bacteria diluted in DMEM. At 90 min post-infection the inoculum was aspirated and an overlay (DMEM, 5% FCS, 20 μg gentamicin ml^{-1}, 0.5% agarose [Seakem ME]) was added to each well. The second overlay (DMEM, 5% FCS, 20 μg gentamicin ml^{-1}, 0.5% agarose, 0.1% Neutral Red solution [Gibco BRL]) was added at either 24 h or 48 h post-infection and plaque formation observed 6-8 h later. Plaques were in general visible without staining at 48 h.

Indirect immunofluorescence of whole bacteria. Indirect immunofluorescence labelling of bacteria was performed as described previously (May & Morona, 2008). Briefly, equivalent numbers of mid exponential-phase bacteria were fixed in formalin (3.7% (v/v) paraformaldehyde in 0.85% saline) and either centrifuged onto poly-L-lysine-coated coverslips for microscopic analysis or kept in suspension for flow cytometric analysis. Bacteria were incubated with the desired primary antibody diluted 1:100 in PBS with 10% foetal calf serum (FCS) prior to washing with PBS and labelling with either an Alexa 488-

181 conjugated donkey anti-rabbit or Alexa 488-conjugated donkey anti-mouse secondary

182 antibody (Molecular Probes). Microscopy was performed as described previously (May &

183 Morona, 2008), using an Olympus IX-70 microscope with phase-contrast optics using a 100×

184 oil immersion objective and a 1.5× enlarger as required. Fluorescence and phase-contrast

185 images were false colour merged using Metamorph (Version 6.3r7, Molecular devices).

186 Alternatively, after labeling, cells were washed three times in PBS and then diluted to

187 5 ml in PBS for analysis by flow cytometry (BD FACSCanto, BD Biosciences, San Jose, CA,

188 USA).

189 **Infection of tissue culture monolayers with *S. flexneri* and immunofluorescence**

190 **labelling**. Infection of HeLa cells and immunofluorescence labelling were performed as

191 recently described (May & Morona, 2008). Briefly, HeLa cells were inoculated with mid

192 exponential-phase bacteria and incubated for 1 h. The monolayers were washed, incubated

193 with media containing gentamicin for a further 1.5 h. The monolayer was washed, formalin-

194 fixed, and permeabilized with 0.1% Triton X-100. After blocking in 10% FCS the infected

195 cells were incubated with polyclonal anti-*Shigella* LPS-Oag (Denka Seiken Co., Japan) to

196 label bacteria. After subsequent washing, cells were incubated with Alexa 594-conjugated

197 donkey anti-rabbit antibodies (Molecular probes). F-actin was visualised by staining with

198 FITC phalloidin (0.1 μg ml^{-1}, Sigma).

199

200 **RESULTS**

201 *In situ* **chemical cross-linking of IcsA**. In order to determine if IcsA is present within a

202 protein complex, *in situ* chemical cross-linking was performed. Mid exponential-phase

203 cultures of *S. flexneri* Δ*icsA* [pIcsA] (RMA2090, Table 1) were treated with membrane-

204 permeable cross-linking agents dithio-bis(succinimidylpropionate) (DSP), and whole-cell

205 lysates were subjected to SDS-PAGE and Western blotting with an anti-IcsA antibody. We

206 reproducibly detected the presence of a high molecular weight (HMW) complex following

207 cross-linking (Fig. 1, lane 2). This complex had an apparent molecular mass greater than 460

208 kDa, as determined by comparison to HighMark protein standard (Invitrogen). Formation of

209   this HMW product was reversed by the addition of β-mercaptoethanol, which can cleave the

210   disulphide bond in the spacer arm of DSP to allow separation of the cross-linked products

211   (Fig. 1, lane 1). This HMW complex could also be detected following cross-linking with

212   formaldehyde (Fig S1 in the supplemental material).

213   Oligomerization of the *N. gonorrhea* IgA protease and *E. coli* AIDA has been

214   suggested to be mediated through interaction of individual translocation domains (Müller *et*

215   *al.*, 2005; Veiga *et al.*, 2002). We examined previously characterized IcsA effector domain

216   deletion mutants (Suzuki *et al.*, 1996) for formation of HMW complexes. DSP crosslinking

217   of IcsA$_{\Delta508\text{-}730}$ (RMA2208) or IcsA$_{\Delta103\text{-}507}$ (RMA2209) produced HMW products,

218   comparable to IcsA$_{WT}$ (RMA2205) (Fig. 1, lanes 3-6). These data indicated that no individual

219   region within IcsA$_{103\text{-}730}$ is alone responsible for formation of the HMW complex; we cannot

220   exclude that multiple interactions within this region are involved. Alternately, the data

221   indicate that IcsA HMW complex formation may be mediated by a region outside of the

222   studied deletions, namely by the translocation domain (IcsA$_{758\text{-}1102}$).

223   Lipopolysaccharide (LPS) is a major constituent of the OM of Gram-negative bacteria

224   consisting of three major parts - the lipid A, the core polysaccharide, and the O antigen (Oag)

225   polysaccharide chain. The Oag component of LPS has been shown to influence both IcsA

226   function and surface localization, restricting the protein to the cell pole (Hong & Payne,

227   1997; Morona & Van Den Bosch, 2003a, b; Sandlin *et al.*, 1994). Rough LPS (R-LPS)

228   lacking the Oag component, was reported to allow IcsA diffusion away from the cell pole

229   (Robbins *et al.*, 2001). We hypothesized that cross-linking of IcsA into a HMW product may

230   be dependent on the spatial confinement of IcsA proteins to the pole or be facilitated by

231   lateral LPS-IcsA interactions. Hence, we examined the IcsA complex formation in the

232   absence of LPS-Oag. HMW IcsA-related complexes were observed following DSP cross-

233   linked of IcsA expressed in the rough LPS strain *S. flexneri* Δ*icsA* Δ*rmlD* [pIcsA]

234   (RMA2107), indicating that complex formation occurred independent of LPS-Oag (Fig. S1).

235

Co-immunoprecipitation of epitope-tagged IcsA proteins. Chemical cross-linking had indicated the presence of IcsA within a HMW complex and we were particularly interested in determining if IcsA is able to self-associate. We applied reciprocal co-purification of differentially epitope-tagged IcsA proteins to determine whether IcsA-IcsA interactions were taking place within this putative complex.

Sites permissive for epitope insertion within the IcsA passenger domain had been previously identified (May & Morona, 2008). The IcsA$_{i87}$ protein has a 5 amino acid linker-insertion at amino acid 87 and when expressed in *S. flexneri*, was found to be comparable to wild-type (IcsA$_{WT}$) with respect to: (i) levels of production; (ii) polar localization at the bacterial surface; and (iii) function, determined by assaying plaque formation on HeLa cell monolayers as a measure of intercellular spreading ability (May & Morona, 2008). Consequently, *icsA*$_{i87}$ was chosen for epitope tagging by exploiting a unique *Not*I restriction site within the linker. Either a synthetic FLAG epitope (DYKDDDDK), or BIO epitope (GLNDIFEAQKIEWH; a substrate for metabolic biotinylation by the BirA biotin-protein ligase; (Cull & Schatz, 1999), were introduced into *icsA*$_{i87}$ as described in the Methods.

E. coli UT5600 strains expressing both epitope-tagged IcsA proteins together (IcsA$_{i87::FLAG}$ and IcsA$_{i87::BIO}$; MG157, Table 1), or tagged proteins individually with control IcsA$_{WT,}$ were generated (MG250 and MG251, Table 1). Overexpression of BirA increased the levels of biotinylated IcsA$_{i87::BIO}$, while retaining the high specificity of the biotinylation reaction (data not shown). Hence, all co-expression strains additionally carried plasmid pCY216 that expressed the *birA* enzyme (Chapman-Smith *et al.*, 1994). Insertion of neither the FLAG nor the BIO epitope affected the function of IcsA$_{i87}$ (data not shown).

The OM fractions of the co-expression strains were isolated and purification strategies directed against either epitope were performed independently: FLAG M2 resin was used for purification of IcsA$_{i87::FLAG}$; and streptavidin-Dynabeads were used for purification of biotinyl-IcsA$_{i87::BIO}$. Co-purification of tagged IcsA proteins was assessed by Western blotting using either an antibody conjugate (FLAG epitope) or streptavidin conjugates (biotin-modified BIO epitope) in each of the eluents. Following purification of IcsA$_{i87::FLAG}$

264   with FLAG M2 resin from OMs of strain MG157, biotinyl-IcsA$_{i87::BIO}$ was found to co-purify

265   with it (Fig. 2a, lane 2). Taking into consideration that any IcsA$_{i87::BIO}$ that remained

266   unbiotinylated could not be detected with streptavidin, our data suggests the amount of co-

267   purified biotinyl-IcsA$_{i87::BIO}$ we observed was significant. Under the same conditions, when

268   OMs of strain MG251 that expressed IcsA$_{WT}$ were used, biotinyl-IcsA$_{i87::BIO}$ was not detected

269   in the eluted sample (Fig. 2a, lane 1) showing that the FLAG M2 resin was specific for the

270   FLAG epitope. Similarly, when biotinyl-IcsA$_{i87::BIO}$ was purified from OMs of strain MG157

271   using streptavidin-Dynabeads, IcsA$_{i87::FLAG}$ was found to co-purify with it (Fig. 2b, lane 2).

272   However, under the same conditions, IcsA$_{i87::FLAG}$ did not purify from OMs of strain MG250

273   that co-expressed the untagged control protein IcsA$_{WT}$ (Fig. 2b, lane 3), showing that the

274   streptavidin-Dynabeads were specific for the biotin-modified BIO epitope. Based on these

275   results we conclude that the IcsA self-association occurs in the OM and this self-association

276   is resistant to disruption by the detergent Zwittergent 3-14.

277

278   **Identification of negative-dominant IcsA$_i$ mutants.** Having detected the existence of IcsA-

279   IcsA interactions by co-purification, we investigated if IcsA self-association impacted on its

280   function in intracellular motility. We hypothesized the existence of IcsA mutations that

281   would exert negative dominance on IcsA function in ABM and intercellular spread when co-

282   expressed with IcsA$_{WT}$. A collection of IcsA$_i$ insertion mutants has been previously identified

283   (May & Morona, 2008) and some of these were screened for negative dominance in

284   intercellular spreading when co-expressed with IcsA$_{WT}$ in a *S. flexneri* KMRM254

285   background (data not shown). Two mutants (IcsA$_{i563}$, and IcsA$_{i677}$) exerted a clear negative

286   dominant phenotype when expressed with either IcsA$_{WT}$ (Fig. 3a) or the functionally

287   equivalent IcsA$_{i87::FLAG}$ (Fig. S2). Individually, IcsA$_{i563}$ and IcsA$_{i677}$ are unable to recruit N-

288   WASP (Fig. S3) or efficiently generate F-actin tails and promote plaque formation on HeLa

289   cell monolayers (May & Morona, 2008). When either mutant was co-expressed with IcsA$_{WT}$,

290   F-actin tails could still detected by FITC-phalloidin staining of fixed monolayers infected

291   with the various *Shigella* strains (Fig. 3b). However, efficient F-actin tail formation is

292   required for efficient intercellular spreading. As a sensitive measure of the proficiency of the

293   detected F-actin tails to drive intercellular spreading, the ability of the co-expression strains

294   to form plaques on HeLa cell monolayers was assessed. Plaque formation could not be

295   detected when $IcsA_{i563}$ was co-expressed with $IcsA_{WT}$ and co-expression of $IcsA_{i677}$ with

296   $IcsA_{WT}$ resulted in only a few small plaques (<1 mm diameter) that were markedly smaller

297   than those formed by the control strain KMRM255 (which typically formed between 50-100

298   plaques/well, averaging 6.4 mm in diameter) (Fig. 3a). The defective plaque formation

299   clearly indicated that the F-actin tails formed by these strains were not comparable to wild-

300   type, as they were not able to facilitate efficient ABM and intercellular spreading.

301

302   **Negative dominance of $IcsA_i$ mutants on $IcsA_{WT}$ does not arise due to defects in**

303   **production, export or polar localization of the wild-type protein.** The observation of

304   negative dominance when $IcsA_{WT}$ was expressed with $IcsA_i$ mutants could have arisen by

305   titration by the mutant proteins of factors required for IcsA synthesis, polar localisation and

306   surface presentation, resulting in a decrease-in-function of $IcsA_{WT}$. We sought to scrutinise

307   these possibilities by using a tagged version of $IcsA_{WT}$ ($IcsA_{i87::FLAG}$) in *S. flexneri* Δ*icsA*

308   strains additionally expressing $IcsA_{i563}$ or $IcsA_{i677}$ mutants. $IcsA_{i87::FLAG}$ retains wild-type

309   equivalent function in plaque formation (Fig. S2 in the supplemental material). We confirmed

310   that the $IcsA_{i563}$ and $IcsA_{i677}$ mutants had a negative dominant effect on $IcsA_{i87::FLAG}$ with

311   respect to plaque formation (Fig. S2).

312   The levels of $IcsA_{i87::FLAG}$ protein during co-expression with $IcsA_{i563}$ and $IcsA_{i677}$,

313   were then assessed by Western blotting with anti-FLAG M2 antibodies. $IcsA_{i87::FLAG}$

314   production was equivalent when expressed alone from either plasmid pKMRM250 (pBR233-

315   derivative) or plasmid pKMRM270 (pBBR1MCS2-derivative), confirming the suitability of

316   the plasmids for use in co-expression studies (not shown). Production of $IcsA_{i87::FLAG}$ when

317   co-expressed with $IcsA_{WT}$ in KMRM275 was comparable to production of $IcsA_{i87::FLAG}$ when

318   expressed alone in KMRM273 (Table 1; Fig. 4a). Despite being unable to form detectable

319   plaques, the strain co-expressing $IcsA_{i677}$ with $IcsA_{i87::FLAG}$ expressed comparable levels of

320 FLAG-tagged functional IcsA; co-expression of $IcsA_{i563}$ and $IcsA_{i87::FLAG}$ resulted in a slight

321 decrease in FLAG-tagged IcsA (Fig. 4a). Additionally, we quantitated the level of surface

322 exposed $IcsA_{i87::FLAG}$ by flow cytometry. Co-expression of $IcsA_{i87::FLAG}$ with either mutant did

323 not result in a detectable reduction in the amount of functional protein at the bacterial surface

324 (Fig. 4b). Moreover, the surface distribution of $IcsA_{i87::FLAG}$ was seen by immunofluorescence

325 to be polar when co-expressed either with $IcsA_{WT}$, $IcsA_{i563}$, or $IcsA_{i677}$ (Fig. 4c).

326   Taken together, these data suggest that the negative dominant phenotype conferred by

327 $IcsA_{i563}$ and $IcsA_{i677}$ during co-expression with active IcsA results from a net functional

328 defect at the cell surface, and was not due to these mutants affecting the expression, export or

329 localisation of functional IcsA proteins.

330

331 **DISCUSSION**

332 Subversion of the host cell actin regulatory network enables *Shigellae* infection to spread

333 throughout the human intestinal epithelium. IcsA is both necessary and sufficient to

334 potentiate actin-based motility through activation of N-WASP. The nature of IcsA interaction

335 with N-WASP remains poorly understood. In light of data demonstrating that the

336 conventional AT, IgA protease from *N.gonorrhoea*, forms an oligomer in the OM, we sought

337 to characterize the properties of IcsA in the OM. In this study, we tested the hypothesis that

338 IcsA is able to self-associate.

339   The self-association of IcsA was supported by the presence of HMW IcsA-related

340 complexes that were detected following cross-linking of whole cells with DSP or

341 formaldehyde. While IgA1 protease *in vitro* oligomerization was reported as homo-

342 pentameric (Veiga *et al.*, 2002), our findings do not exclude the possibility that IcsA

343 oligomerization is hetero-oligomeric. The reciprocal co-purification and genetic interaction

344 data we have presented in this study strongly suggests the existence of IcsA-IcsA interactions

345 within the HMW oligomer.

346   Support for the existence of direct IcsA-IcsA interactions within HMW complexes

347 was provided by observation of negative dominant genetic interactions of $IcsA_i$ linker-

348   insertion mutants ($IcsA_{i563}$ and $IcsA_{i677}$) on IcsA function in intercellular spreading (assessed

349   with both $IcsA_{WT}$ and $IcsA_{i87::FLAG}$). One of two explanations can account for negative

350   dominant phenotypes (Herskowitz, 1987). The first is titration of factors away from the

351   functional IcsA protein by co-expression of a mutants $IcsA_i$ protein. Since no defects were

352   observed in functional IcsA whole-cell protein levels, in cell surface expression, or in polar

353   targeting, the factors that underpin the respective processes were not titrated by $IcsA_i$

354   mutants. Similarly, the examined $IcsA_i$ mutants cannot recruit N-WASP (May & Morona,

355   2008), and titration of this host cell ligand from functional IcsA was improbable. These

356   findings indicated that titration could not explain the negative dominant phenotype. Instead,

357   we favour the alternate explanation of negative dominance: that the products of the functional

358   *icsA* and mutant *icsA_i* alleles functionally interact *in vivo*. We suggest that during co-

359   expression, $IcsA_i$ mutants are included into mixed complexes with functional IcsA proteins.

360   The inclusion of $IcsA_i$ proteins renders these complexes defective for efficient F-actin tail

361   formation, as evidenced by defective intercellular spreading. This deficiency in the negative

362   dominant co-expression strains occurs despite levels of functional IcsA that, when expressed

363   alone, can efficiently potentiate intercellular spreading. Clearly, IcsA-IcsA interactions are

364   functionally important.

365   We have demonstrated for the first time biochemical and genetic evidence of IcsA

366   self-association. Furthermore, the observed negative dominance of certain inactive $IcsA_i$

367   mutant proteins is consistent with self-association being important for the biological function

368   of the protein. Although N-WASP and WASP family members are activated by an array of

369   different molecules, these activators act by allosteric relief of N-WASP/WASP auto-

370   inhibition (Kim *et al.*, 2000), and by facilitating clustering and multimerization of active N-

371   WASP (Padrick *et al.*, 2008; Padrick & Rosen, 2010), often by their own oligomerization.

372   Therefore, we hypothesise the self-association of IcsA may play a role in N-WASP

373   clustering. In our study the incorporation of defective $IcsA_{i563}$ or $IcsA_{i677}$ proteins into

374   $IcsA_{WT}$-containing complexes could interfere with efficient spatial clustering of activated N-

375   WASP, thereby accounting for the reduced efficiency of intercellular spreading. In this way,

376   IcsA would appear analogous to other bacterial and host proteins that either interact with or

377   functionally mimic WASP family members. Most of these have been shown to either directly

378   self-associate (Enterohaemorrhagic *Escherichia coli* intimin-tir), to spatially cluster (*Listeria*

379   *monocytogenes* ActA)   or   are   inherently   multivalent   with   internal   repeats

380   (Enterohaemorrhagic *Escherichia coli* EspF, EspF$_U$ and Tccp) (Alto *et al.*, 2007; Campellone

381   *et al.*, 2008; Footer *et al.*, 2008; Sallee *et al.*, 2008; Touzé *et al.*, 2004). Significantly, our

382   data demonstrates self-association of yet another protein known to activate a WASP family

383   protein, which has emerged as an important feature in the regulation of the host actin-

384   cytoskeleton.

385

REFERENCES

Alto, N. M., Weflen, A. W., Rardin, M. J., Yarar, D., Lazar, C. S., Tonikian, R., Koller, A., Taylor, S. S., Boone, C., & other authors. **(2007).** The type III effector EspF coordinates membrane trafficking by the spatiotemporal activation of two eukaryotic signaling pathways. *J Cell Biol* **178**, 1265–1278.

Barnard, T. J., Dautin, N., Lukacik, P., Bernstein, H. D. & Buchanan, S. K. (2007). Autotransporter structure reveals intra-barrel cleavage followed by conformational changes. *Nat Struct Mol Biol* **14**, 1214–1220.

Bernardini, M. L., Mounier, J., d'Hauteville, H., Coquis-Rondon, M. & Sansonetti, P. J. (1989). Identification of *icsA*, a plasmid locus of *Shigella flexneri* that governs bacterial intra- and intercellular spread through interaction with F-actin. *Proc Natl Acad Sci USA* **86**, 3867–3871.

Campellone, K. G., Cheng, H.-C., Robbins, D., Siripala, A. D., McGhie, E. J., Hayward, R. D., Welch, M. D., Rosen, M. K., Koronakis, V. & Leong, J. M. (2008). Repetitive N-WASP-binding elements of the enterohemorrhagic *Escherichia coli* effector EspF(U) synergistically activate actin assembly. *PLoS Pathog* **4**, e1000191.

Chapman-Smith, A., Turner, D. L., Cronan, J. E., Morris, T. W. & Wallace, J. C. (1994). Expression, biotinylation and purification of a biotin-domain peptide from the biotin carboxy carrier protein of *Escherichia coli* acetyl-CoA carboxylase. *Biochem J* **302 (3)**, 881–887.

Cotter, S. E., Surana, N. K. & St Geme, J. W. (2005). Trimeric autotransporters: a distinct subfamily of autotransporter proteins. *Trends Microbiol* **13**, 199–205.

Cull, M. G. & Schatz, P. J. (1999). Biotinylation of proteins *in vivo* and *in vitro* using small peptide tags. *Meth Enzymol* **326**, 430–440.

Enninga, J., Mounier, J., Sansonetti, P. J. & Tran Van Nhieu, G. (2005). Secretion of

422   type III effectors into host cells in real time. *Nat Methods* **2**, 959–965.

423 **Footer, M. J., Lyo, J. K. & Theriot, J. A. (2008).** Close packing of *Listeria monocytogenes*
424   ActA, a natively unfolded protein, enhances F-actin assembly without dimerization. *J*
425   *Biol Chem* **283**, 23852–23862.

426 **Gangwer, K. A., Mushrush, D. J., Stauff, D. L., Spiller, B., McClain, M. S., Cover, T. L.**
427   **& Lacy, D. B. (2007).** Crystal structure of the *Helicobacter pylori* vacuolating toxin p55
428   domain. *Proc Natl Acad Sci USA* **104**, 16293–16298.

429 **Goldberg, M. B. (2001).** Actin-based motility of intracellular microbial pathogens.
430   *Microbiol Mol Biol Rev* **65**, 595–626.

431 **Henderson, I. R., Navarro-Garcia, F., Desvaux, M., Fernandez, R. C. & Ala'Aldeen, D.**
432   **(2004).** Type V protein secretion pathway: the autotransporter story. *Microbiol Mol Biol*
433   *Rev* **68**, 692–744.

434 **Herskowitz, I. (1987).** Functional inactivation of genes by dominant negative mutations.
435   *Nature* **329**, 219–222.

436 **Hong, M. & Payne, S. M. (1997).** Effect of mutations in *Shigella flexneri* chromosomal and
437   plasmid-encoded lipopolysaccharide genes on invasion and serum resistance. *Mol*
438   *Microbiol* **24**, 779–791.

439 **Hritonenko, V., Kostakioti, M. & Stathopoulos, C. (2006).** Quaternary structure of a
440   SPATE autotransporter protein. *Mol Membr Biol* **23**, 466–474.

441 **Jain, S. & Goldberg, M. B. (2007).** Requirement for YaeT in the outer membrane assembly
442   of autotransporter proteins. *J Bacteriol* **189**, 5393.

443 **Kim, A. S., Kakalis, L. T., Abdul-Manan, N., Liu, G. A. & Rosen, M. K. (2000).**
444   Autoinhibition and activation mechanisms of the Wiskott-Aldrich syndrome protein.
445   *Nature* **404**, 151–158.

446 **Klemm, P., Vejborg, R. M. & Sherlock, O. (2006).** Self-associating autotransporters,
447   SAATs: functional and structural similarities. *Int J Med Microbiol* **296**, 187–195.

448 **Kotloff, K. L., Noriega, F., Losonsky, G. A., Sztein, M. B., Wasserman, S. S., Nataro, J.**
449   **P. & Levine, M. M. (1996).** Safety, immunogenicity, and transmissibility in humans of
450   CVD 1203, a live oral *Shigella flexneri* 2a vaccine candidate attenuated by deletions in
451   *aroA* and *virG*. *Infect Immun* **64**, 4542–4548.

452 **Kotloff, K. L., Taylor, D. N., Sztein, M. B., Wasserman, S. S., Losonsky, G. A., Nataro,**
453   **J. P., Venkatesan, M., Hartman, A., Picking, W. D., & other authors**. **(2002).** Phase I
454   evaluation of Δ*virG Shigella sonnei* live, attenuated, oral vaccine strain WRSS1 in
455   healthy adults. *Infect Immun* **70**, 2016–2021.

456 **Kovach, M. E., Elzer, P. H., Hill, D. S., Robertson, G. T., Farris, M. A., Roop, R. M. &**
457   **Peterson, K. M. (1995).** Four new derivatives of the broad-host-range cloning vector
458   pBBR1MCS, carrying different antibiotic-resistance cassettes. *Gene* **166**, 175–176.

459 **Lett, M. C., Sasakawa, C., Okada, N., Sakai, T., Makino, S., Yamada, M., Komatsu, K.**
460   **& Yoshikawa, M. (1988).** *virG*, a plasmid-coded virulence gene of *Shigella flexneri*:
461   identification of the VirG protein and determination of the complete coding sequence. *J*
462   *Bacteriol* **171**, 353–359.

463 **Levine, M. M., Kotloff, K. L., Barry, E. M., Pasetti, M. F. & Sztein, M. B. (2007).**
464   Clinical trials of *Shigella* vaccines: two steps forward and one step back on a long, hard
465   road. *Nat Rev Microbiol* **5**, 540–553.

466 **Lugtenberg, B., Meijers, J., Peters, R., van der Hoek, P. & van Alphen, L. (1975).**
467   Electrophoretic resolution of the "major outer membrane protein" of *Escherichia coli*
468   K12 into four bands. *FEBS Lett* **58**, 254–258.

469 **Makino, S., Sasakawa, C., Kamata, K., Kurata, T. & Yoshikawa, M. (1986).** A genetic
470   determinant required for continuous reinfection of adjacent cells on large plasmid in *S.*

471   *flexneri* 2a. *Cell* **46**, 551–555.

472 **Marín, E., Bodelón, G. & Fernández, L. A. (2010).** Comparative analysis of the
473   biochemical and functional properties of C-terminal domains of autotransporters. *J*
474   *Bacteriol* **192**, 5588–5602.

475 **May, K. L. & Morona, R. (2008).** Mutagenesis of the *Shigella flexneri* autotransporter IcsA
476   reveals novel functional regions involved in IcsA biogenesis and recruitment of host
477   neural Wiscott-Aldrich syndrome protein. *J Bacteriol* **190**, 4666–4676.

478 **Meng, G., Spahich, N., Kenjale, R., Waksman, G. & St Geme, J. W. (2011).** Crystal
479   structure of the *Haemophilus influenzae* Hap adhesin reveals an intercellular
480   oligomerization mechanism for bacterial aggregation. *EMBO J* **30**, 3864–3874.

481 **Miki, H. & Takenawa, T. (2003).** Regulation of actin dynamics by WASP family proteins. *J*
482   *Biochem* **134**, 309–313.

483 **Morona, R., Daniels, C. & Van Den Bosch, L. (2003).** Genetic modulation of *Shigella*
484   *flexneri* 2a lipopolysaccharide O antigen modal chain length reveals that it has been
485   optimized for virulence. *Microbiol* **149**, 925–939.

486 **Morona, R. & Van Den Bosch, L. (2003a).** Lipopolysaccharide O antigen chains mask IcsA
487   (VirG) in *Shigella flexneri*. *FEMS Microbiol Lett* **221**, 173–180.

488 **Morona, R. & Van Den Bosch, L. (2003b).** Multicopy *icsA* is able to suppress the virulence
489   defect caused by the *wzz*(SF) mutation in *Shigella flexneri*. *FEMS Microbiol Lett* **221**,
490   213–219.

491 **Müller, D., Benz, I., Tapadar, D., Buddenborg, C., Greune, L. & Schmidt, M. A. (2005).**
492   Arrangement of the translocator of the autotransporter adhesin involved in diffuse
493   adherence on the bacterial surface. *Infect Immun* **73**, 3851–3859.

494 **Oomen, C. J., van Ulsen, P., van Gelder, P., Feijen, M., Tommassen, J. & Gros, P.**
495   **(2004).** Structure of the translocator domain of a bacterial autotransporter. *EMBO J* **23**,
496   1257–1266.

497 **Padrick, S. B., Cheng, H.-C., Ismail, A. M., Panchal, S. C., Doolittle, L. K., Kim, S.,**
498   **Skehan, B. M., Umetani, J., Brautigam, C. A., & other authors**. **(2008).** Hierarchical
499   regulation of WASP/WAVE proteins. *Mol Cell* **32**, 426–438.

500 **Padrick, S. B. & Rosen, M. K. (2010).** Physical mechanisms of signal integration by WASP
501   family proteins. *Annu Rev Biochem* **79**, 707–735.

502 **Pallen, M. J., Chaudhuri, R. R. & Henderson, I. R. (2003).** Genomic analysis of secretion
503   systems. *Curr Opin Microbiol* **6**, 519–527.

504 **Peterson, J. H., Tian, P., Ieva, R., Dautin, N. & Bernstein, H. D. (2010).** Secretion of a
505   bacterial virulence factor is driven by the folding of a C-terminal segment. *Proc Natl*
506   *Acad Sci USA* **107**, 17739–17744.

507 **Prossnitz, E., Nikaido, K., Ulbrich, S. J. & Ames, G. F. (1988).** Formaldehyde and
508   photoactivatable cross-linking of the periplasmic binding protein to a membrane
509   component of the histidine transport system of *Salmonella typhimurium*. *J Biol Chem*
510   **263**, 17917–17920.

511 **Robbins, J. R., Monack, D., McCallum, S. J., Vegas, A., Pham, E., Goldberg, M. B. &**
512   **Theriot, J. (2001).** The making of a gradient: IcsA (VirG) polarity in *Shigella flexneri*.
513   *Mol Microbiol* **41**, 861–872.

514 **Sallee, N. A., Rivera, G. M., Dueber, J. E., Vasilescu, D., Mullins, R. D., Mayer, B. J. &**
515   **Lim, W. A. (2008).** The pathogen protein EspF(U) hijacks actin polymerization using
516   mimicry and multivalency. *Nature* **454**, 1005–1008.

517 **Sandlin, R. C., Lampel, K. A., Keasler, S. P., Goldberg, M. B., Stolzer, A. L. & Maurelli,**
518   **A. T. (1994).** Avirulence of rough mutants of *Shigella flexneri*: requirement of O antigen
519   for correct unipolar localization of IcsA in the bacterial outer membrane. *Infect Immun*

520   **63**, 229–237.

521 **Sansonetti, P. J., Arondel, J., Fontaine, A., d'Hauteville, H. & Bernardini, M. L. (1991).**
522   *OmpB* (osmo-regulation) and *icsA* (cell-to-cell spread) mutants of *Shigella flexneri*:
523   vaccine candidates and probes to study the pathogenesis of shigellosis. *Vaccine* **9**, 416–
524   422.

525 **Snapper, S. B., Takeshima, F., Antón, I., Liu, C. H., Thomas, S. M., Nguyen, D., Dudley,**
526   **D., Fraser, H., Purich, D., & other authors**. **(2001).** N-WASP deficiency reveals
527   distinct pathways for cell surface projections and microbial actin-based motility. *Nat Cell*
528   *Biol* **3**, 897–904.

529 **Suzuki, T., Miki, H., Takenawa, T. & Sasakawa, C. (1998).** Neural Wiskott-Aldrich
530   syndrome protein is implicated in the actin-based motility of *Shigella flexneri*. *EMBO J*
531   **17**, 2767–2776.

532 **Suzuki, T., Mimuro, H., Suetsugu, S., Miki, H., Takenawa, T. & Sasakawa, C. (2002).**
533   Neural Wiskott-Aldrich syndrome protein (N-WASP) is the specific ligand for *Shigella*
534   VirG among the WASP family and determines the host cell type allowing actin-based
535   spreading. *Cell Microbiol* **4**, 223–233.

536 **Suzuki, T., Saga, S. & Sasakawa, C. (1996).** Functional analysis of *Shigella* VirG domains
537   essential for interaction with vinculin and actin-based motility. *J Biol Chem* **271**, 21878–
538   21885.

539 **Swanson, K. A., Taylor, L. D., Frank, S. D., Sturdevant, G. L., Fischer, E. R., Carlson,**
540   **J. H., Whitmire, W. M. & Caldwell, H. D. (2009).** *Chlamydia trachomatis*
541   polymorphic membrane protein D is an oligomeric autotransporter with a higher-order
542   structure. *Infect Immun* **77**, 508–516.

543 **Thanabalu, T., Koronakis, E., Hughes, C. & Koronakis, V. (1998).** Substrate-induced
544   assembly of a contiguous channel for protein export from *E. coli*: reversible bridging of
545   an inner-membrane translocase to an outer membrane exit pore. *EMBO J* **17**, 6487–6496.

546 **Touzé, T., Hayward, R. D., Eswaran, J., Leong, J. M. & Koronakis, V. (2004).** Self-
547   association of EPEC intimin mediated by the beta-barrel-containing anchor domain: a
548   role in clustering of the Tir receptor. *Mol Microbiol* **51**, 73–87.

549 **Van Den Bosch, L., Manning, P. A. & Morona, R. (1997).** Regulation of O-antigen chain
550   length is required for *Shigella flexneri* virulence. *Mol Microbiol* **23**, 765–775.

551 **Van Den Bosch, L. & Morona, R. (2003).** The actin-based motility defect of a *Shigella*
552   *flexneri rmlD* rough LPS mutant is not due to loss of IcsA polarity. *Microb Pathogenesis*
553   **35**, 11–18.

554 **Veiga, E., Sugawara, E., Nikaido, H., de Lorenzo, V. & Fernández, L. A. (2002).** Export
555   of autotransported proteins proceeds through an oligomeric ring shaped by C-terminal
556   domains. *EMBO J* **21**, 2122–2131.

557 **Xicohtencatl-Cortes, J., Saldaña, Z., Deng, W., Castañeda, E., Freer, E., Tarr, P. I.,**
558   **Finlay, B. B., Puente, J. L. & Girón, J. A. (2010).** Bacterial macroscopic rope-like
559   fibers with cytopathic and adhesive properties. *J Biol Chem* **285**, 32336–32342.

560 **Yarar, D., To, W., Abo, A. & Welch, M. D. (1999).** The Wiskott-Aldrich syndrome protein
561   directs actin-based motility by stimulating actin nucleation with the Arp2/3 complex.
562   *Curr Biol* **9**, 555–558.

563

564
565

TABLE 1. Bacterial strains and plasmids used

Strain/Plasmid	Relevant characteristics *	Reference/source
E. coli K-12		
DH5α	*endA hsdR supE44 thi-1 recA1 gyrA relAΔ* (*lacZYA-argF*) U169 [φ80 d*lac*Δ (*lacZ*) *M15*] *phoA*	Gibco-BRL
UT5600	F⁻ *ara-14 leuB6 secA6 lacY1 proC14 tsx-67* Δ(*ompT-fepC*)*266 entA403 trpE38 rfbD1 rpsL109 xyl-5 mtl-1 thi-1*	Laboratory collection
MG157	UT5600 [pKMRM270, pMG55, pCY216]	This study
MG250	UT5600 [pKMRM270, pKMRM1, pCY216]	This study
MG251	UT5600 [pKMRM252, pMG55, pCY216]	This study
S. flexneri		
2457T	*S. flexneri* 2a wild-type	Laboratory collection
RMA2041	2457T Δ*icsA*::Tc^R	(Van Den Bosch & Morona, 2003)
RMA2090	RMA2041 [pIcsA]	(Van Den Bosch & Morona, 2003)
RMA2107	RMA2041 Δ*rmlD*::Km^R [pIcsA]	(Van Den Bosch & Morona, 2003)
RMA2205	RMA2041 [pD10-1]	This study
RMA2208	RMA2041 [pD10-1 *virG3*]	This study
RMA2209	RMA2041 [pD10-1 *virG4*]	This study
KMRM111	RMA2041 [pKMRM11]	(May & Morona, 2008)
KMRM134	RMA2041 [pKMRM34]	(May & Morona, 2008)
KMRM254	RMA2041 [pKMRM252]	This study
KMRM255	RMA2041 [pKMRM252] [pIcsA]	This study
KMRM256	RMA2041 [pKMRM252] [pKMRM11]	This study
KMRM258	RMA2041 [pKMRM252] [pKMRM34]	This study
KMRM273	RMA2041 [pKMRM270]	This study
KMRM275	RMA2090 [pKMRM270]	This study
KMRM276	RMA2041 [pKMRM11] [pKMRM270]	This study
KMRM277	RMA2041 [pKMRM34] [pKMRM270]	This study
Plasmids		
pBBR1MCS-2	Broad-host-range vector; Km^K; medium copy no.; *ori* compatible with ColE1 plasmids	(Kovach *et al.*, 1995)
pCY216	encodes BirA; Cm^R	(Chapman-Smith *et al.*, 1994)
pD10-1	encodes VirG (same as IcsA$_{WT}$); Tp^R	(Suzuki *et al.*, 1996)
pD10-1*virG3*	encodes VirG$_{\Delta508-730}$; Tp^K	(Suzuki *et al.*, 1996)
pD10-1*virG4*	encodes VirG$_{\Delta103-507}$; Tp^K	(Suzuki *et al.*, 1996)
pIcsA	*icsA* gene cloned into pBR322; Ap^R	(Van Den Bosch & Morona, 2003)
pKMRM1	pBR322 encoding IcsA$_{i87}$; Ap^R	(May & Morona, 2008)
pKMRM11	pBR322 encoding IcsA$_{i563}$; Ap^K	(May & Morona, 2008)

pKMRM34	pBR322 encoding IcsA$_{i677}$; Ap^R	(May & Morona, 2008)
pKMRM250	pBR322 encoding IcsA$_{i87::FLAG}$; Ap^R	This study
pKMRM252	pBBR1MCS-2 encoding IcsA$_{WT}$; Km^R	This study
pKMRM270	pBBR1MCS-2 encoding IcsA$_{i87::FLAG}$; Km^R	This study
pMG55	pBR322 encoding IcsA$_{i87::BIO}$; Ap^R	This study

568   * Cm^R, chloramphenicol-resistant; Tc^R, tetracyline-resistant; Km^R, kanamycin-resistant; Ap^R, ampicillin-
569   resistant; Tp^R, trimethroprim-resistant.

570

TABLE 2. Oligonucleotides

Oligo	Sequence (5' - 3')*
KM1_BIO_F	**GGCC**TGAACGACATCTTCGAAGCTCAGAAAATCGAATGGCAC
KM1_BIO_R	**GGCCG**TGCCATTCGATTTTCTGAGCTTCGAAGATGTCGTTCA
IcsA_FLAG_F1	**GGCC**GCGACTACAAGGACGATGACGACAAG
IcsA_FLAG_R1	**GGCCC**TTGTCGTCTACGTCCTTGTAGTCGC

* Bold nucleotides comprise the *Not*I overhang of the annealed epitopes.

FIG. 1. DSP cross-linking of *S. flexneri*. Mid-exponential phase cultures of indicated *S. flexneri* strains were treated with 0.2 mM DSP as described in the Methods. Whole membranes were isolated and resuspended in sample buffer with or without β-mercaptoethanol (β-ME) and heated to 60°C. Cross-linked samples were resolved by SDS PAGE (7.5% polyacrylamide) and analysed by Western blotting with anti-IcsA antibody. Sizes were approximated from the electrophoretic mobility of HighMark (Invitrogen) protein standard. Expected electrophoretic migration of monomeric IcsA truncation mutants is indicated. IcsA* indicates HMW complexes containing IcsA. The resolving gel is shown.

FIG. 2. Co-purification analysis. *E. coli* K-12 strains (MG157, MG250, MG251) were grown, then Zwittergent 3-14-solubilised OM fractions were prepared and purified through FLAG-agarose resin (a) or streptavidin-Dynabeads (b), as described in the Methods. Samples were subjected to SDS-PAGE, and Western blotting with either a rabbit anti-FLAG M2 antibody followed with an anti-rabbit Ig HRP conjugate, or streptavidin-HRP, as indicated.

FIG. 3. Plaque and F-actin tail formation by complemented strains. (a) Relative size and frequency of plaque formation on HeLa cell monolayers by *S. flexneri* strains expressing either $IcsA_{WT}$ (RMA2090), or $IcsA_{i563}$ (KMRM111), or $IcsA_{i677}$ (KMRM134) alone, and *S. flexneri* co-expressing $IcsA_{WT}$ with $IcsA_{i563}$ (KMRM256), $IcsA_{i677}$ (KMRM258), or $IcsA_{WT}$ control (KMRM255). Plaque assay was performed as described in detail in the materials and methods. **(b)** IF microscopy of F-actin tail formation by intracellular *S. flexneri* strains expressing either $IcsA_{WT}$ (RMA2090), or $IcsA_{i563}$ (KMRM111), or $IcsA_{i677}$ (KMRM134) alone, and *S. flexneri* co-expressing $IcsA_{WT}$ with $IcsA_{i563}$ (KMRM256), $IcsA_{i677}$ (KMRM258), or $IcsA_{WT}$ control (KMRM255). HeLa cells infected with *S. flexneri* were labelled with anti-LPS antibodies and Alexa 594-conjugated donkey anti-rabbit antibodies, and F-actin was labelled with FITC phalloidin as described in detail in the Methods. Strains were assessed in three independent experiments. Arrows indicate F-actin tails. Scale bar = 10 μm.

FIG. 4. Protein levels and distribution of IcsA$_{i87::FLAG}$ during co-expression with IcsA$_{i563}$ and IcsA$_{i677}$ mutants. (A) Whole-cell lysates from mid exponential-phase cultures of indicated *S. flexneri* strains expressing IcsA$_{i87::FLAG}$ with IcsA$_{i563}$ (KMRM276), IcsA$_{i677}$ (KMRM277), or control IcsA$_{WT}$ (KMRM275) were subjected to Western blotting with anti-FLAG antibodies. The samples represent 1×10^{8} cells. IcsA'$_{i87::FLAG}$ is a proteolytic fragment also observed in IcsA$_{WT}$. (B) FACS analysis of the indicated *S. flexneri* strains. Equivalent numbers of bacteria were labelled with rabbit anti-FLAG and then anti-rabbit-Alexa 488 antibodies, and fluorescence intensity assessed by flow cytometry as described in the Material and Methods. Grey area denotes fluorescence intensities of the negative control strain (KMRM250). For all strains, n = 50,000 cells. (C) IF microscopy of IcsA$_{i87::FLAG}$ surface distribution. Mid exponential-phase cultures of indicated *S. flexneri* strains were formalin fixed and labelled with anti-FLAG antibodies and then goat anti-rabbit Alexa 488 secondary antibodies. Scale bar = 3 μm.
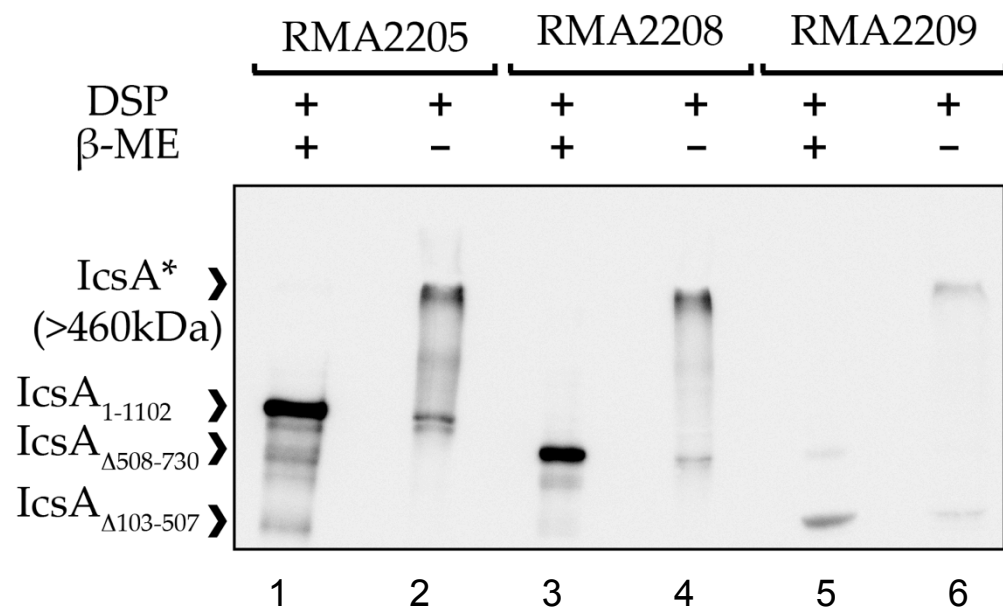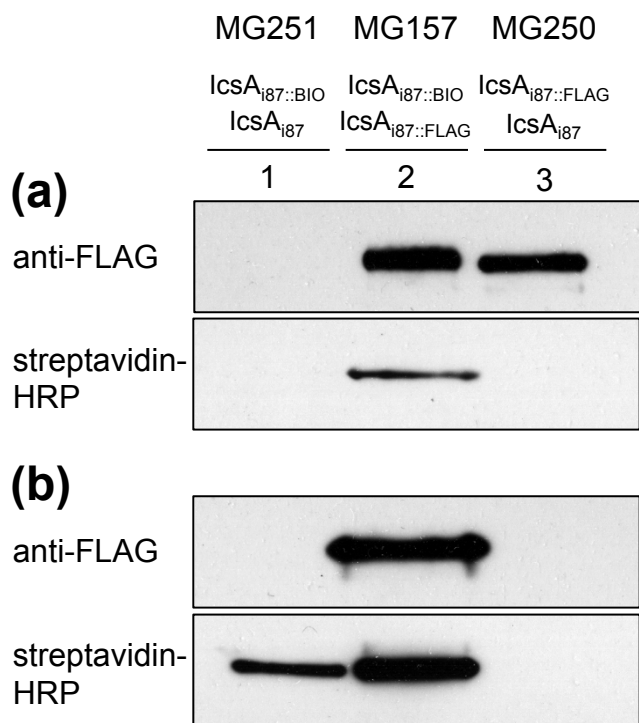
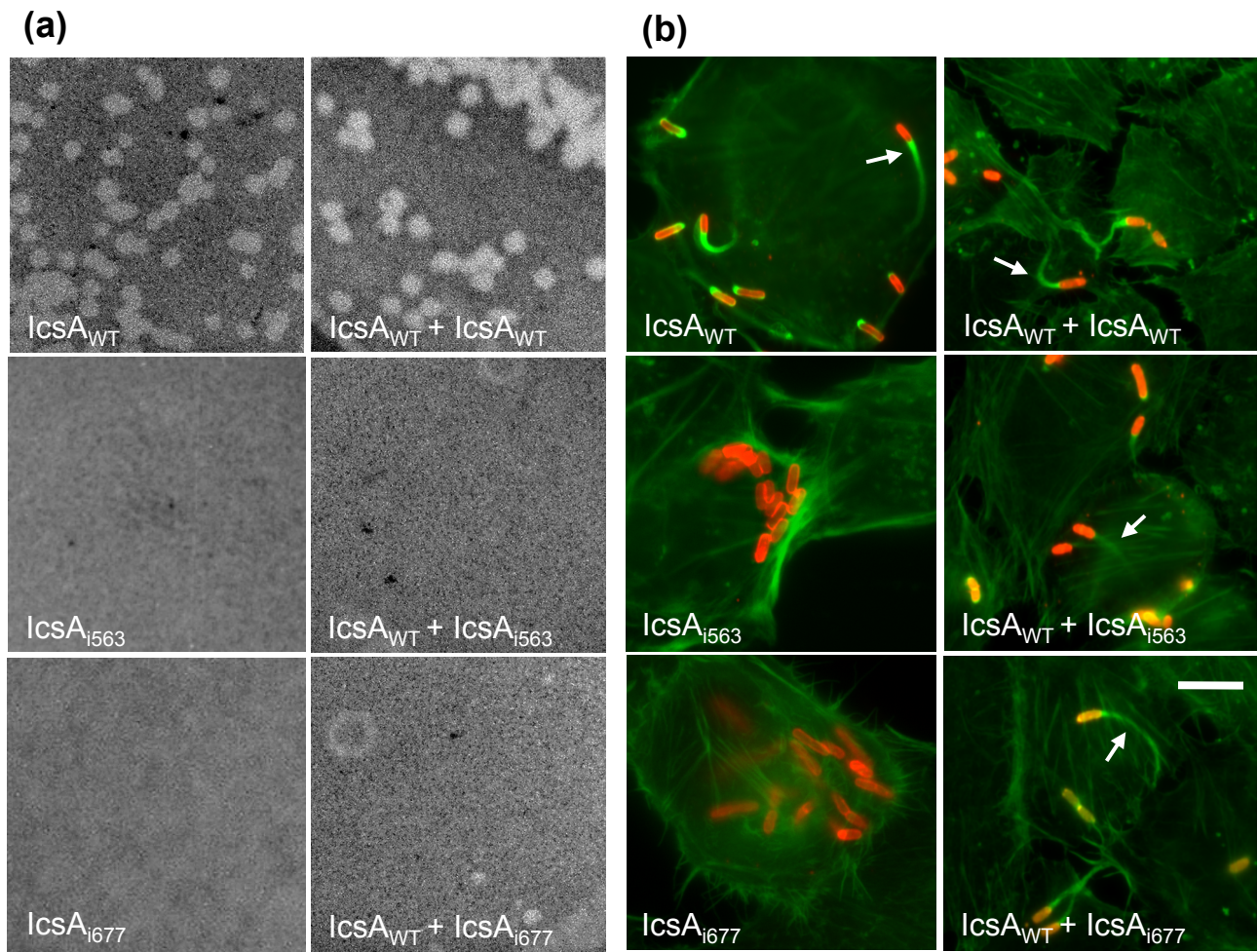FIG. 1. DSP cross-linking of *S. flexneri*.

FIG. 2. Co-purification analysis

(a)

IcsA$_{WT}$ | IcsA$_{WT}$ + IcsA$_{WT}$

IcsA$_{i563}$ | IcsA$_{WT}$ + IcsA$_{i563}$

IcsA$_{i677}$ | IcsA$_{WT}$ + IcsA$_{i677}$

(b)

IcsA$_{WT}$ | IcsA$_{WT}$ + IcsA$_{WT}$

IcsA$_{i563}$ | IcsA$_{WT}$ + IcsA$_{i563}$

IcsA$_{i677}$ | IcsA$_{WT}$ + IcsA$_{i677}$

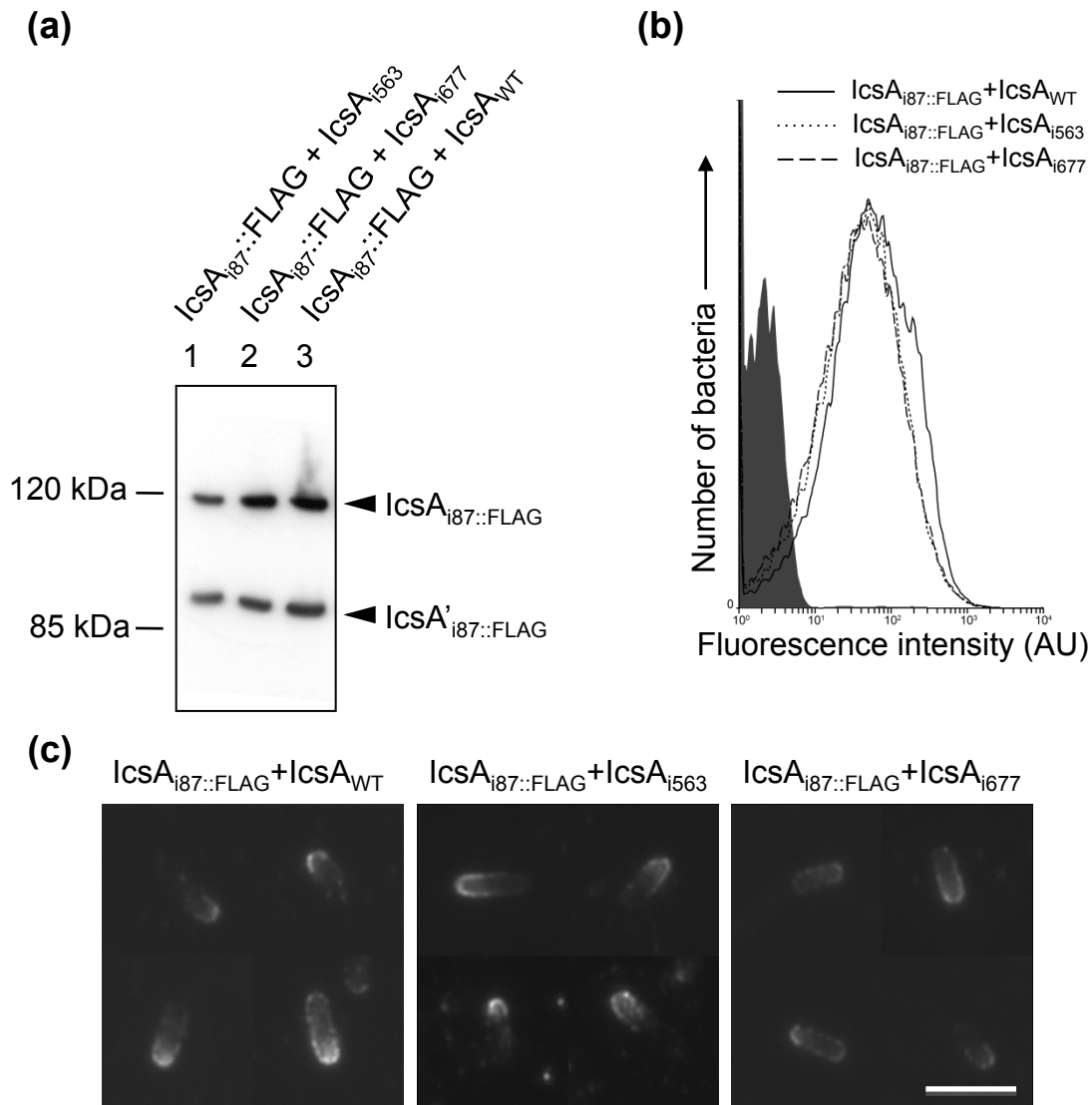FIG. 3. Plaque and F-actin tail formation by complemented strains

FIG. 4. Protein levels and distribution of IcsA$_{i87::FLAG}$ during co-expression with IcsA$_{i563}$ and IcsA$_{i677}$ mutants.